Mechanism of the 10-methylacridinium ion-sensitized photooxidation of *N*,*N*-dibenzylhydroxylamine and its derivatives in acetonitrile

Yasuhiro Ohba,[a] Kanji Kubo,[b] Tetsutaro Igarashi[a] and Tadamitsu Sakurai*[a]

[a] *Department of Applied Chemistry, Faculty of Engineering, Kanagawa University, Kanagawa-ku, Yokohama 221-8686, Japan*
[b] *Institute of Advanced Material Study, 86, Kyushu University, Kasuga-koen, Kasuga, Fukuoka 816-0811, Japan*

Received (in Cambridge, UK) 16th November 2000, Accepted 27th February 2001
First published as an Advance Article on the web 20th March 2001

The 10-methylacridinium ion (MA^+)-sensitized photooxidation of substituted *N*,*N*-dibenzylhydroxylamines (**1**) in acetonitrile occurred mainly by a superoxide ion mechanism to give *N*-benzylidenebenzylamine *N*-oxides (**2**) and hydrogen peroxide quantitatively. Analysis of substituent effects on the limiting quantum yield for formation of **2** showed that back electron transfer (ET) from the 10-methylacridinyl radical ($MA^{\bullet}$) to the radical cation $\mathbf{1}^{+\bullet}$ proceeds in the Marcus 'normal region'. In addition, this back ET was found to take place in preference to one-electron reduction of O_2 by $MA^{\bullet}$.

Introduction

Much attention has been devoted to the electron transfer-initiated photooxygenation reactions of various electron-rich alkenes, including aromatic compounds, from synthetic and mechanistic points of view,[1] whereas there are only a few studies regarding the photosensitized oxidations of hydroxylamines.[2] In previous studies we demonstrated that the cyano-substituted anthracene-sensitized photooxidation of substituted *N*,*N*-dibenzylhydroxylamines (**1**) is a good system for exploring the mechanism of the oxidation reaction of hydroxylamines initiated by electron transfer (ET).[3] An interesting finding in our study is that the limiting quantum yield for the photooxidation is determined by the relative rate of back ET within the initially formed geminate radical ion pair. Since ET from **1** to a salt as a sensitizer induces no net charge separation, we might be able to enhance the formation of free hydroxylamine radical cations and, hence, to lower the relative rate for back ET, compared with ET to cyano-substituted anthracenes.[4] In order to find out the factors that control the sensitized photooxidation efficiency of hydroxylamines, we chose 10-methylacridinium perchlorate (MAP) as an ET-type photosensitizer and **1a**–**f** as substrates and investigated substituent effects on the MAP-sensitized photooxidation of **1** in acetonitrile (MeCN).

Results and discussion

An O_2-purged MeCN solution of **1b** (1.0×10^{-3} mol dm^{-3}) containing MAP (5.0×10^{-4} mol dm^{-3}) was irradiated for 3.5 h with light of wavelength longer than 340 nm at room temperature. ^{1}H NMR analysis of the product mixture using *N*-(1-naphthylidene)-1-naphthylmethylamine *N*-oxide as an internal standard revealed that *N*-benzylidenebenzylamine *N*-oxide (**2b**) is formed in 97% yield when 62% of the starting **1a** is consumed and MAP remains unchanged. No change in the MAP concentration is further substantiated by the finding that the UV absorption of MAP undergoes negligible change during irradiation in the wavelength range 330–460 nm. Hydrogen peroxide was also found to be obtained in 100% yield by iodometry of the same reaction mixture. In addition, the absorption spectrum of each product has a maximum around 300 nm, where MAP exhibits only weak absorption. This is in agreement with the absorption spectrum of the corresponding authentic sample **2** (Scheme 1). Control experiments showed that the oxidation of **1** occurs to a negligible extent without either MAP or O_2.

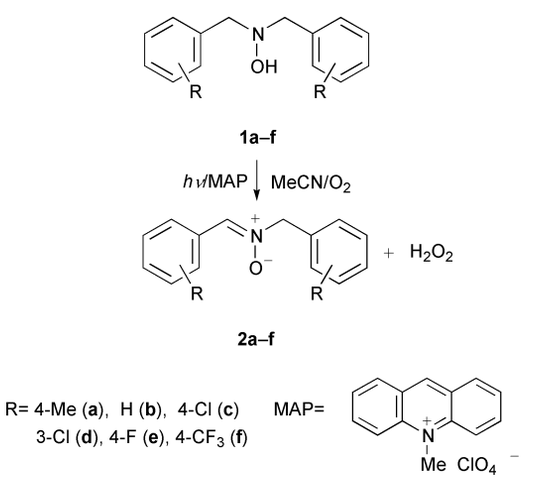

Scheme 1

A typical plot given in Fig. 1 demonstrates that the fluorescence of MAP is quenched by **1** according to the Stern–Volmer equation $I_0/I = 1 + k_{et}\tau_S[\mathbf{1}]$, where I and I_0 are the fluorescence intensities of MAP with and without **1**, respectively, k_{et} is the bimolecular quenching rate constant, and τ_S is the fluorescence lifetime of MAP in the absence of **1** (36.2 ns). From the slopes (quenching constants) obtained from the linear plots, the k_{et} values for **1a**–**f** as quenchers were estimated (Table 1). To confirm the occurrence of the MAP emission quenching by ET, the free energy changes for ET ($\Delta_{et}G$) from **1a**–**f** to the excited singlet-state MAP were calculated on the basis of the simplified Weller equation[5] $\Delta_{et}G$/kJ mol^{-1} = $96.5(E_{ox} - E_{red}) - E_S$, where E_{ox} is the oxidation potential of **1** (Table 1), E_{red} is the reduction potential of MAP (−0.43 V *vs.*

DOI: 10.1039/b009206l

Table 1 Free energy changes for ET ($\Delta_{et}G$ and $\Delta_{et}'G$), fluorescence quenching constants ($k_{et}\tau_S$), limiting quantum yield for formation of **2** ($\Phi_{2,lim}$) and related parameters (E_{ox}, k_{et} and $k_{et}'^{Rel}$) in the MAP-sensitized photooxidation of **1** in MeCN

Compound	E_{ox} [a]/V *vs.* SCE	$k_{et}/10^{10}$ M^{-1} s^{-1}	$\Delta_{et}G$/kJ mol^{-1}	$\Phi_{2,lim}$	$k_{et}\tau_S$ [b]/M^{-1}	$k_{et}\tau_S$ [c]/M^{-1}	$k_{et}'^{Rel}$	$\Delta_{et}'G$/kJ mol^{-1}
1a	0.67	1.3	−159	0.049 ± 0.003	470	120	0.37	−106
1b	0.76	1.2	−151	0.019 ± 0.001	450	210	1.0	−115
1c	0.76	1.2	−151	0.0073 ± 0.0003	420	270	2.6	−115
1d	0.85	1.1	−142	0.0083 ± 0.0005	400	120	2.3	−124
1e	0.88	1.1	−139	0.012 ± 0.001	400	220	1.6	−126
1f	1.00	0.80	−127	0.0046 ± 0.0003	290	160	4.2	−138

[a] Previous data (see ref. 3*b*). [b] Determined from the fluorescence quenching of MAP by **1**. [c] Estimated from the dependence of Φ_2 on the concentration of **1**. 1 M = 1 mol dm^{-3}.

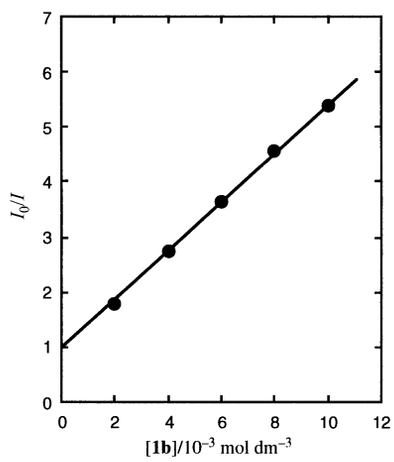

Fig. 1 Stern–Volmer plot for the fluorescence quenching of MAP (1.0×10^{-4} mol dm^{-3}) by **1b** in N_2-saturated MeCN at room temperature. Excitation wavelength is 366 nm.

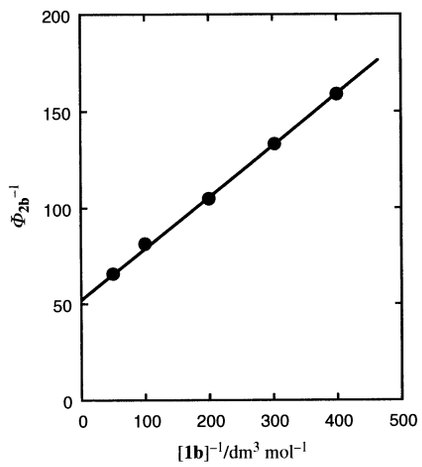

Fig. 2 Plot of Φ_{2b}^{-1} *versus* $[\mathbf{1b}]^{-1}$ for the photooxidation of **1b** in the presence of MAP (1.0×10^{-4} mol dm^{-3}) in O_2-purged MeCN at room temperature. Irradiation wavelength is 366 nm.

SCE in MeCN)[6], and E_S is the first singlet excitation energy of MAP (265 kJ mol^{-1}).[6] These are collected in Table 1. The magnitude of the $\Delta_{et}G$ values evaluated, therefore, leads us to conclude that the fluorescence quenching occurs by an ET mechanism.

Since no induction of net charge separation by ET to the excited-state MAP strongly suggests that solvent cage effects play a minor role, we are able to propose Scheme 2 (in which

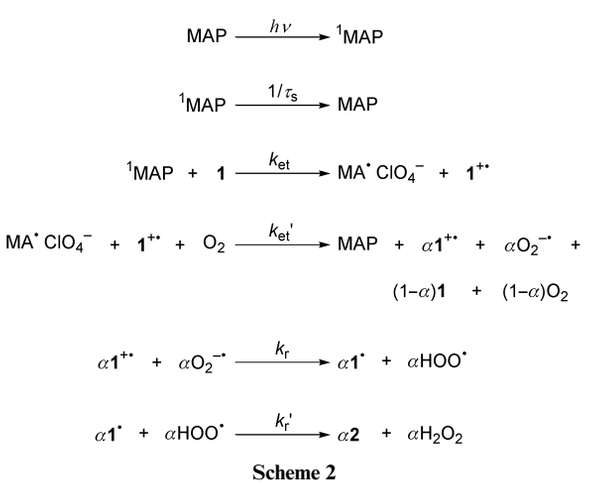

Scheme 2

superoxide ion is involved as the major oxidizing species in the process) on the basis of the results described above. Application of the steady-state approximation to Scheme 2 gives eqn. (1),

$$1/\Phi_2 = (1/a)\{1 + 1/(k_{et}\tau_S[\mathbf{1}])\} \quad (1)$$

where Φ_2 refers to the quantum yield for the formation of **2** and a is the ratio of ET to O_2 to the overall ET (to **1**$^{+\bullet}$ and O_2). The fortunate observation that the product **2** exhibits strong UV absorption around 300 nm (where only the weak absorption of MAP is detected) made it possible to determine Φ_2 spectrophotometrically at very low conversions of **1** (<1%). As shown in Fig. 2, we obtained linear plots of $1/\Phi_2$ against the reciprocal of the concentration of **1** (1/[**1**]) and then estimated the limiting quantum yields for the appearance of **2** ($\Phi_{2,lim} = a$) and the quenching constants ($k_{et}\tau_S$) from the intercept and the ratio of the intercept to the slope of these linear plots, respectively (Table 1). Comparison of the $k_{et}\tau_S$ values determined according to the two different procedures confirms that the quenching constant estimated from the concentration dependence of Φ_2 is comparable to that obtained by the MAP fluorescence quenching. This finding also substantiates the ET mechanism that is shown in Scheme 2. On the other hand, an inspection of substituent effects on the limiting quantum yield reveals that $\Phi_{2,lim}$ is smaller than that of the cyano-substituted anthracene-sensitized photooxidation by about an order of magnitude, but has a clear tendency to decrease as the electron-withdrawing ability of the substituent R is increased.[3] Because $\Phi_{2,lim}$ is equal to a, the observed poor oxidation efficiency is due to the much slower rate of ET [$k_{et}'(O_2)$] from the 10-methylacridinyl radical (MA$^\bullet$) to O_2 than that of back ET [$k_{et}'(\mathbf{1}^{+\bullet})$] to **1**$^{+\bullet}$. The ability of MA$^\bullet$ to reduce O_2 is considered to be much lower, compared with the reducing ability of cyano-substituted anthracene-derived radical anions.

It has been shown previously that back ET from the 9,10-dicyanoanthracene (DCA)-derived radical anion to **1**$^{+\bullet}$ takes place in the Marcus 'normal region' and its rate is not very sensitive to the electronic effects of the substituent R.[3b] Since we may assume that the ET rate $k_{et}'(O_2)$ undergoes no substituent effects, the equation: $\Phi_{2,lim} = a = k_{et}'(O_2)/[k_{et}'(O_2) + k_{et}'(\mathbf{1}^{+\bullet})]$ allows us to derive eqn. (2). The $k_{et}'^{Rel}$ values calculated by

$$(\Phi_{2a\text{–}f,lim}^{-1} - 1)/(\Phi_{2b,lim}^{-1} - 1) = k_{et}'(\mathbf{1a}\text{–}\mathbf{f}^{+\bullet})/k_{et}'(\mathbf{1b}^{+\bullet}) = k_{et}'^{Rel} \quad (2)$$

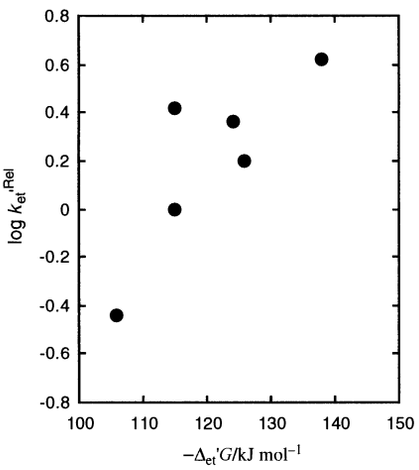

Fig. 3 Relative rate of back electron transfer from the 10-methylacridinyl radical to the radical cation of **1** as a function of the free energy change in MeCN.

using this equation are collected in Table 1. In addition, we evaluated the free energy change for back ET from MA$^{\bullet}$ to **1**$^{+\bullet}$ based on the relation, $\Delta_{et}'G$/kJ mol^{-1} = $-96.5(E_{ox} - E_{red})$ (Table 1). In Fig. 3 is shown the Marcus plot of log $k_{et}^{'Rel}$ *versus* $-\Delta_{et}'G$. The plot clearly indicates that the rate of back ET increases with increasing exothermicity for this process and, hence, leads us to conclude that the ET occurs in the Marcus 'normal region'.[7] This conclusion is consistent with the finding that $\Phi_{2,lim}$ decreases as the electron-withdrawing ability of the substituent R is increased. The much smaller exothermicity of back ET for the MA$^{\bullet}$–**1**$^{+\bullet}$ system than that for the DCA$^{-\bullet}$–**1**$^{+\bullet}$ system may be responsible for a more sensitive dependence of the back ET rate for the former system on $-\Delta_{et}'G$.

Since the possibility of a singlet oxygen mechanism in MeCN still remains, we investigated the solvent deuterium isotope effects on Φ_{2b} using CD_3CN as a solvent in order to estimate the extent to which this mechanism contributes to the overall MAP-sensitized photooxidation of **1**. From eqn. (3)[3] (where D

$$\Phi_{2b}(D)/\Phi_{2b}(H) = \{k_d^1(H) + k_r^1[\mathbf{1b}]\}/\{k_d^1(D) + k_r^1[\mathbf{1b}]\} \quad (3)$$

and H indicate deuteriated and protiated solvents, respectively, k_d^1 is the rate constant for deactivation of singlet oxygen and the rate constant k_r^1 corresponds to the total rate of the reaction between **1b** and singlet oxygen), the quantum yield ratio $\Phi_{2b}(D)/\Phi_{2b}(H)$ for a singlet oxygen mechanism was calculated to be 8.2 and 9.1 at [**1b**] = 2.0×10^{-2} and 0.25×10^{-2} mol dm^{-3}, respectively. A comparison of these calculated isotope effects with the observed isotope effects of 1.2 ± 0.1 ([**1b**] = 2.0×10^{-2} mol dm^{-3}) and 1.9 ± 0.1 ([**1b**] = 0.25×10^{-2} mol dm^{-3}), therefore, confirms that a singlet oxygen mechanism makes only a small contribution, even at low concentrations of **1b**.

Conclusion

Through the analysis of substituent effects on the limiting quantum yield for the appearance of **2**, we found that both the stability of the hydroxylamine radical cation **1**$^{+\bullet}$ and the ability of the 10-methylacridinyl radical to reduce O_2 play key roles in determining the efficiency of the photooxidation reaction of **1**, initiated by ET.

Experimental

UV absorption and fluorescence spectra were recorded on a Shimadzu UV-2200 spectrophotometer and a Shimadzu RF-5000 spectrofluorimeter, respectively. ^{1}H NMR spectra were taken with a JEOL JNM-A500 spectrometer. Chemical shifts were determined using tetramethylsilane as an internal standard. IR spectra were taken with a Hitachi Model 270-30 infrared spectrometer. The fluorescence lifetime of MAP was measured under nitrogen with a time-correlated single-photon counting apparatus (Horiba NAES-700; excitation wavelength = 366 nm; cut-off wavelength = 410 nm), which was equipped with a flash lamp filled with hydrogen. Ten thousand counts were sampled in the peak channel.

Substituted *N*,*N*-dibenzylhydroxylamines (**1a**–**f**) and *N*-benzylidenebenzylamine *N*-oxides (**2a**–**f**) were prepared and purified according to the previously described procedures.[3] Physical and spectroscopic properties of **1** and **2** were consistent with those of previously prepared samples. MAP was prepared according to the method of Roberts *et al*. and purified by recrystallization from methanol.[8] The structure of MAP was established by IR and ^{1}H NMR spectroscopy. Acetonitrile was purified according to the standard method.[9] *N*-(1-Naphthylidene)-1-naphthylmethylamine *N*-oxide, used as an internal standard, was the same as that employed in a previous study.[10] CD_3CN and $CDCl_3$ (Aldrich) were used as received.

A potassium tris(oxalato)ferrate(III) actinometer was employed to determine the quantum yields for the appearance of **2** at low conversions of the starting hydroxylamine **1** (<1%).[11] A 1% conversion of **1** ([**1**] = $2.5–20 \times 10^{-3}$ mol dm^{-3}) into **2** corresponds to a change in the absorbance of 0.45–4.6 around 300 nm, because **2** in MeCN has a molar absorption coefficient of $1.8–2.3 \times 10^4$ dm^3 mol^{-1} cm^{-1} around this wavelength.[3b] A 450 W high-pressure Hg lamp was used as the light source from which 366 nm light was selected with Corning 0-52, Corning 7-60, and Toshiba IRA-25S glass filters. The previously determined molar absorption coefficients of **2a**–**f** were utilized to quantify the formation of **2**.[3b] All of the quantum yields are an average of more than five determinations. Quantitative iodometric analysis of H_2O_2 produced was carried out by using the linear calibration curve for this peroxide, obtained under the same analytical conditions.

References

1 P. S. Mariano and J. L. Stavinoha, in *Synthetic Organic Photochemistry*, ed. W. M. Horspool, Plenum Press, New York, 1984, pp. 145–257.
2 (*a*) G. Pandey, G. Kumaraswamy and A. Krishna, *Tetrahedron Lett.*, 1987, **28**, 2649; (*b*) M. V. Encinas, E. Lemp and E. A. Lissi, *J. Chem. Soc., Perkin Trans. 2*, 1987, 1125; (*c*) P. Bilski, A. S. W. Li and C. F. Chignell, *Photochem. Photobiol.*, 1991, **54**, 345.
3 (*a*) T. Sakurai, Y. Uematsu, O. Tanaka and H. Inoue, *J. Chem. Soc., Perkin Trans. 2*, 1992, 2163; (*b*) T. Sakurai, M. Yokono, K. Komiya, Y. Masuda and H. Inoue, *J. Chem. Soc., Perkin Trans. 2*, 1994, 2515.
4 M. A. Miranda and H. García, *Chem. Rev.*, 1994, **94**, 1063.
5 (*a*) D. Rehm and A. Weller, *Isr. J. Chem.*, 1970, **8**, 259; (*b*) D. Rehm and A. Weller, *Z. Phys. Chem.*, 1970, **69**, 183.
6 S. Fukuzumi, S. Kuroda and T. Tanaka, *J. Chem. Soc., Chem. Commun.*, 1986, 1553.
7 R. A. Marcus, *Annu. Rev. Phys. Chem.*, 1964, **15**, 155.
8 (*a*) R. M. G. Roberts, D. Ostovic and M. M. Kreevoy, *Faraday Discuss. Chem. Soc.*, 1982, **74**, 257; (*b*) M. Fujita and S. Fukuzumi, *J. Chem. Soc., Perkin Trans. 2*, 1993, 1915.
9 J. A. Riddick, W. B. Bunger and T. K. Sakano, *Organic Solvents*, 4th edn., Wiley, Chichester, 1986.
10 Y. Ohba, K. Kubo and T. Sakurai, *J. Photochem. Photobiol. A: Chem.*, 1998, **113**, 45.
11 C. G. Hatchard and C. A. Parker, *Proc. R. Soc. London, A*, 1956, **235**, 518.